

CRITICAL CURRENT BEHAVIOR AND OXIDE BARRIER PROPERTIES OF Ta SURFACE LAYERS ON Nb

S.T. Ruggiero and G.B. Arnold
University of Notre Dame
Notre Dame, IN 46556

and

E. Track and D.E. Prober
Yale University
P.O. BOX 2157
New Haven, CT 06520

Abstract

We have investigated the critical current, $I_c R$, and oxide barrier shape in Nb/Ta/Ox/C.E. tunnel junctions. Here, layers of Ta in the thickness range $0 < D_{Ta} < 1000 \text{ \AA}$ were deposited, in situ, on 2000 \AA thick Nb underlayers. Junctions were completed with Pb, PbBi, and Ag counter-electrodes. We find that as D_{Ta} is increased, there is a more rapid decrease of $I_c R$ compared with the effective energy gap, in accord with an extended version of the Gallagher theory¹ including strong-coupling and electron-scattering effects. In addition, we have investigated the average barrier height, $\bar{\phi}$, and width, s , of the oxide barriers which form on the Ta overlayers. It is observed empirically that $\bar{\phi} \sim 6/(s-s_0)$ where $s_0 \sim 10 \text{ \AA}$ and $\bar{\phi}$ is measured in eV. This relationship is also found to hold for barrier formation on a wide variety of pure and composite metallic systems. These results are discussed in conjunction with the Fromhold-Mott-Cabrera theory² for self-limiting oxide growth on metal surfaces.

Introduction

In this paper we discuss the critical current and oxide barrier properties of tunnel junctions with base electrodes comprising Ta surface layers on Nb. As previously discussed, Ta^{3,4} and a number of other metals⁵⁻⁹ with desirable oxidation properties have been deposited on Nb to form high quality tunnel junctions.

However, along with the improvement in I-V characteristics come an associated decrease in the energy gap and $I_c R$ product and a strong change in oxide barrier properties. A study of the systematics of these effects in Ta overlayer systems on Nb is discussed.

Experimental

The junctions were prepared by depositing thin Ta overlayers, in situ, on 2000 \AA Nb films by ion-beam deposition as previously discussed.³ In order to prepare a series of samples each with a different Ta thickness and an identical Nb/Ta interface, a sample holder was employed which sequentially shuttered up to 5 samples after the Ta deposition had been initiated. After deposition, and ~ 30 min. had elapsed to allow internal cryogenically cooled surfaces to warm, the chamber was either vented with room air, or first brought to ~ 1 -2 Torr with pure oxygen for 3-4 minutes. The samples were then transferred to a thermal evaporation chamber (within ~ 12 minutes) wherein 2000 \AA of Ge was deposited on samples through a wire mask to insulate base electrode edges and define a $75 \mu\text{m}$ line. To create $75 \mu\text{m} \times 75 \mu\text{m}$ area junctions a second Ge deposition was made orthogonal to the first. Otherwise (and

more typically) $75 \mu\text{m} \times 350 \mu\text{m}$ junctions were made by depositing counterelectrodes through a mechanically slotted mask. Ag, Pb, and 29 wt. % Bi PbBi films were used to complete the junctions.

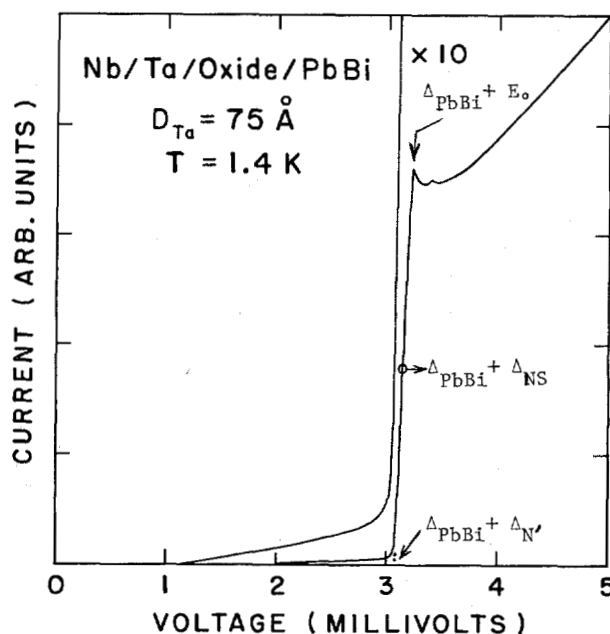


Fig. 1. Current-voltage curves for a tunnel junction with a base electrode comprising 75 \AA Ta on 2000 \AA Nb.

Energy Gap and $I_c R$ Product

Surface layers on Nb, while providing sharp, low leakage I-V characteristics, can also have a strong effect on junction characteristics in the vicinity of the sum gap. Since overlayer materials characteristically have T_c 's less than that of Nb, any overlayer metal remaining after oxidation will form a proximity system with the underlying Nb. As discussed by Arnold and Wolf,¹⁰ because of the lower pair potential, Δ_{Ta} , in the surface layer compared with that of Nb, Δ_N , and consequent Andreev scattering at the N/S boundary, a bound quasi-particle state will be created in the surface layer. This effect is clearly evident in Fig. 1 for a junction with 75 \AA Ta on Nb, the bound state being manifest as a clear peak or "knee" at an energy $E_0 + \Delta_{PbBi}$. The position of this peak, which decreases in energy with increasing overlayer thickness, D_N , sets an upper limit on the effective energy gap of the system. In addition, as discussed by

Gallagher,¹ as D_N increases there should also be a coincident and proportionally more rapid decrease in the $I_C R$ product in the vicinity of $D_N = 0$.

Shown in Fig. 2 are the results for a variety of gap parameters and the measured $I_C R$ products of a series of Nb/Ta/Ox/C.E. junctions with varying Ta overlayer thickness, D_{Ta} . Plotted are E_0 , defined as the peak position on the proximity "knee" minus Δ_{PbBi} and also, for reference, the effective energy gap, Δ_{NS} and the energy at which conduction first occurs, Δ_N' , defined here as the point of maximum slope and the extrapolated voltage intercept, respectively, of the rising I-V characteristic, minus Δ_{PbBi} ($\Delta_{PbBi} = 1.75 \text{ meV}$).

We note that there is a significant decrease of $I_C R$ with junction resistance at fixed D_{Ta} . This interesting behavior has been reported for Si barrier systems as well.¹² Since, for a given system, the $I_C R$ product should be a universal parameter, it has been postulated that, for our junctions, the presence of non-thermal - presumably extrinsic - noise and the increased susceptibility of the junction to this noise as resistance increases, may contribute to this behavior. However, as implied by the measurements of Smith et al.¹² a complete explanation of this behavior in Si barrier junctions may well involve a phenomenon of intrinsic origin, perhaps related to the detailed nature of the tunnel barrier itself. In any case, for our samples, since a measurement on a relatively low-resistance ($7.5 \times 10^{-4} \Omega\text{-cm}^2$) junction was available ($D_{Ta} = 25 \text{ \AA}$, $I_C R = 1.9 \text{ meV}$), this point was plotted as measured and data for differing D_{Ta} were extrapolated to this resistance. We note, however, that for a given (higher) resistance the as-measured data showed a parallel behavior of decreasing $I_C R$ with increasing D_{Ta} .

According to the theory of the proximity effect,¹⁰ the density of states for tunneling into a thin N layer of an N/S proximity sandwich consists of a sharp, non-BCS-like peak at an energy E_0 , due to a quasi-particle bound state. In a clean N layer, there are no states between E_0 and Δ_c , the gap of the underlying superconductor. At Δ_s , the density of states rises sharply from zero to a peak just above Δ_s . When this density of states is convoluted with the BCS density of states of a counter electrode, as in the case for tunneling in our Nb/Ta/Ox/PbBi junctions, the result is a sharp peak at $E_0 + \Delta_c$ (C=PbBi counterelectrode) in the I vs. V curve, as in Fig. 1. (The additional small peak just above $E_0 + \Delta_c$ may be due to a very thin proximity layer in the PbBi counterelectrode, which would produce such a peak at $\Delta_c + \Delta_s$ (S=Nb)).

The energy E_0 can thus be obtained quite accurately in these samples. In theory, it depends on Δ_{Nb} , D_{Ta}/ξ_{Ta} , Δ_{Ta} , r , and d/λ , which are, respectively, the Nb gap, the ratio of Ta thickness to Ta coherence length, the gap induced in the Ta overlayer, the probability amplitude for reflection at the Ta/Nb interface, and the ratio of Ta thickness to mean free path for s-wave elastic scattering in the Ta layer.

The $I_C R$ product, determined from an extended version of the Gallagher theory,¹ also depends on the same parameters, in addition to its dependence on temperature and Δ_{PbBi} , the PbBi gap, both of which are accurately known. The only quantities which are not directly obtained from the experiment are r and d/λ (once r and d/λ are known, Δ_{Ta} is determined, using Δ_{Nb}

and D_{Ta}/ξ_{Ta} , by the equations of the theory,¹⁰ using the bulk α_F and μ^* obtained from tunneling into bulk Ta.¹³

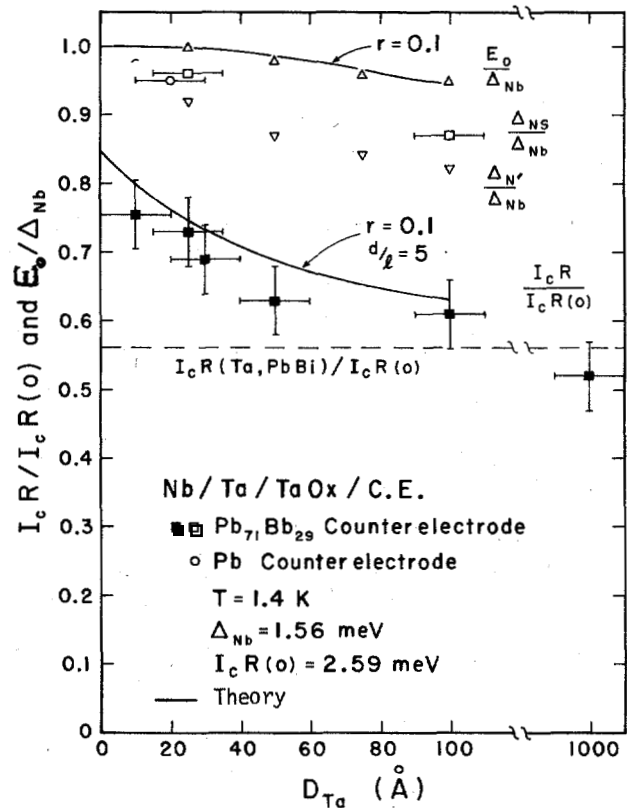


Fig. 2. Reduced gap parameters and $I_C R$ product as a function of Ta surface layer thickness. E_0 , the positions of the bound state conductance peak and the $I_C R$ product have been self-consistently fit with values of the reflection amplitude, r , of 0.1. The theory for $I_C R$ includes both strong coupling and interlayer scattering effects.

Shown in Fig. 2 are theoretical fits to our two experimentally derived parameters, E_0 and $I_C R$, for Ta thicknesses from 10 Å to 1000 Å, using two parameters, r and d/λ . Because of the way in which the junctions were prepared, these two parameters should be nearly the same for all junctions. In our fitting, we found that E_0 is most sensitive to r , so that E_0 determines r which in our case was found to be 0.1, giving a reflection probability $r^2 = .01$. This is approximately what one would calculate for reflection from a step barrier at the Nb/Ta interface, with a height equal to the (small) difference between the Fermi energies of Nb and Ta. The $I_C R$ product showed very little sensitivity to the parameters r and d/λ . Though we chose $d/\lambda = 5$ for the curve in Fig. 2, a choice of $d/\lambda = 1$ uniformly raises the curve by only a slight amount. $I_C R$ is primarily sensitive to Δ_{Nb} , Δ_{PbBi} , and D_{Ta}/ξ_{Ta} , all of which can be determined from experiment. The small offset in the data may represent some residual overall intrinsic suppression or an artifact of our extrapolation procedure.

Tunnel Barrier Properties

It has been observed that the application of surface layers on Nb changes the barrier shape from the

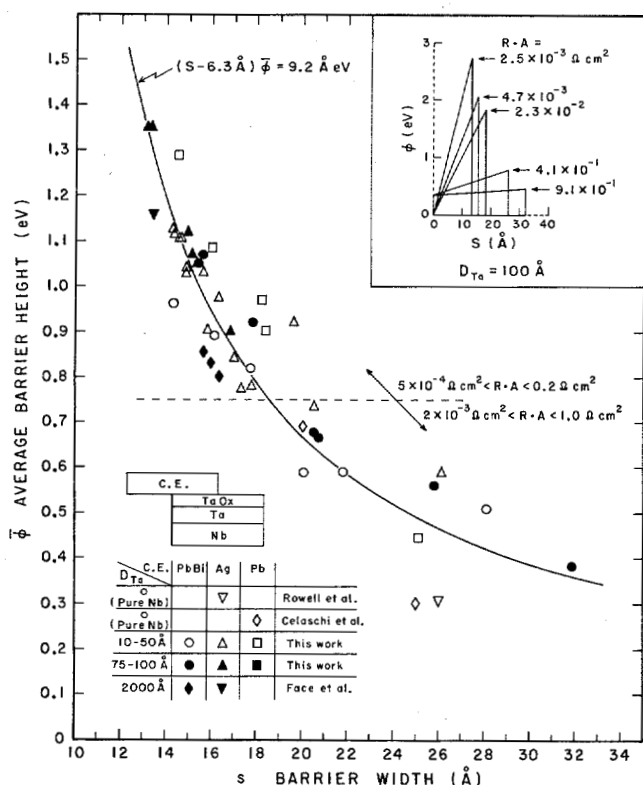


Fig. 3. Average barrier height and width for oxide layers grown on Ta surface layers on Nb, pure Ta, and pure Nb. Junctions shown were completed with a variety of counterelectrode materials. Insert shows the representative shape of barriers on Ta as a function of increasing resistance (oxidation time).

low ($\sim 0.3 \text{ eV}$), broad ($\sim 30 \text{ Å}$) barriers characteristic of pure Nb to much higher ($\sim 1 \text{ eV}$) and narrower ($\sim 20 \text{ Å}$) barriers associated with the surface layer materials themselves. This has been observed in our Ta^{3,4} and for the Al^{5,6} and Zr⁹ overlayer systems. This link between large barrier height and good I-V characteristics is particularly striking in recent results on Nb where Celaschi et al.¹⁴ have shown that under the appropriate deposition conditions high, narrow barriers can be grown on Nb itself and produce characteristics comparable to those achievable in surface layer systems. We have also observed for our Ta overlayers that barrier shape is a function of oxidation time. As shown in the inset of Fig. 3, there is a systematic decrease of the average barrier height with increased oxidation time, that is, with increasing barrier width, s . The dependence of the average barrier height, $\bar{\phi}$, with s , for the data shown in the inset along with those for a variety of Ta thicknesses and counterelectrodes have been plotted in the Figure. It is clear that as oxidation proceeds there is a systematic decrease in $\bar{\phi}$ with s , a trend which is roughly universal and also includes data for pure Ta,¹⁵ and those for both high¹⁴ and low¹⁶ barriers on pure Nb.

To obtain a broader perspective of this behavior, data for a variety of systems available in the literature, which span a large range of $\bar{\phi}$, have been plotted

in Fig. 4, including data for pure Al^{17,18} and Al overlayer systems.¹⁹ It is clear here that both within a given system and for the data in general there is a systematic decrease in measured barrier height with width. As shown, this behavior can be empirically parameterized by $\bar{\phi} \sim 6 \text{ eV}/(s-10 \text{ Å})$. Also shown in the figure are the results from the Fromhold-Mott-Cabrera theory.² This theory describes self-limiting oxide growth on metals wherein there is an initial rapid formation of a thin oxide layer - the growth of which is dominated by ionic diffusion through the oxide and typically represents a major fraction of the final thickness - and the subsequent transition to a much slower growth rate governed principally by electron tunneling. Here, a description of electron tunneling is employed which is similar to the trapezoidal barrier model used to derive $\bar{\phi}$ and s from high bias I-V junction characteristics.^{18,20} As described by the theory, there is an initial potential difference, $V_K = V_M$ (the Mott potential) between the metal and surface-oxide Fermi levels which drives the ion-dominated growth stage. As oxidation proceeds, the oxide Fermi level rises, decreasing V_K . The transition to the slower, electron-dominated growth stage can be defined as the point where $V_K = 0$.

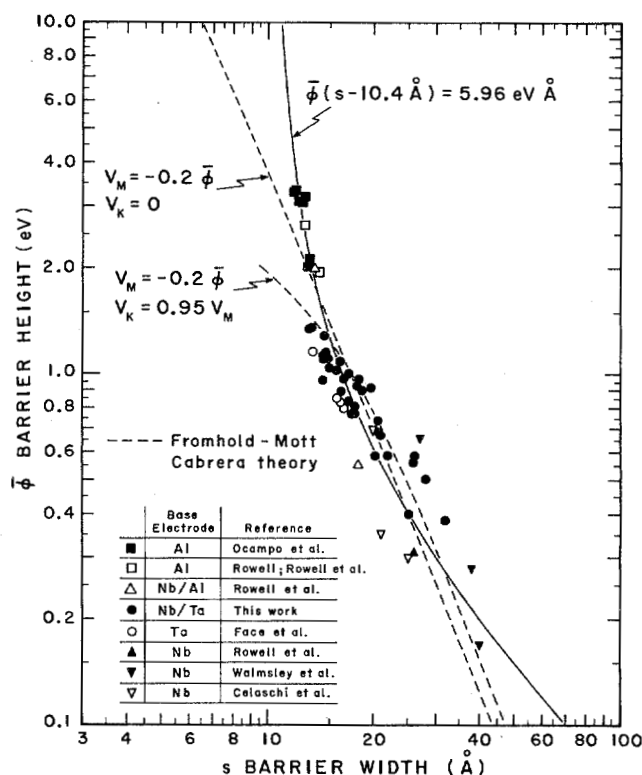


Fig. 4. Average height as a function of width for barriers grown a variety of pure and surface layer systems. Dotted lines show results for the Fromhold-Mott-Cabrera theory for self-limiting oxide growth on metals. Parameters discussed in text.

In Fig. 4, we show calculated values of oxide thickness at this transition point versus average overall barrier height $\bar{\phi}$ and asymmetry V_M .²¹ Also included are the results for a pre-transition thickness defined for $V_K = 0.95 V_M$. Although, as seen in Fig. 3,

the measured barrier asymmetry of completed junctions can vary with $\bar{\phi}$, an average asymmetry taken as 20% of $\bar{\phi}$ ($V_M = -0.2\bar{\phi}$) in conjunction with values of $V_K = 0$ and $0.95 V_M$ represents the obtainable range of theoretical results in the vicinity of the data shown. Because these data encompass a wide variety of materials and oxidation conditions, the transition thickness and barrier parameters for completed junctions will not necessarily be represented by this calculation which is based on barrier shape prior to counterelectrode deposition. We note that the theory tends to predict values of the ionic diffusion constant D_i , (here of 10^{-6} cm²/sec and 10^{-8} cm²/sec for $V_K = 0$ and $V_K = 0.95 V_M$ respectively) which are large in comparison with values implied from post-transition oxide growth studies at elevated temperatures for Nb,¹⁴ Ag²² and Ta.²³ It appears that for a given barrier height, the theory consistently implies oxide thicknesses too large by $\sim 5\text{\AA}$, to compensate for which large values of D_i must be employed (changing D_i tends simply to shift the theoretical curves along the abscissa). Nonetheless, the theory gives a good overall description of the data and we note that a general offset in the calculated barrier width may have its origin in the complex nature of (and potentials present at) the oxide-counterelectrode interface. Experiments combining insitu oxidation and identical base and counterelectrodes, for example, would be especially helpful in a further understanding of this behavior.

Conclusions

We have investigated the behavior of the $I_C R$ product and the general oxidation properties of tunnel junctions containing Ta surface layers on Nb. As suggested by theory,¹ an initial and proportionally more rapid decrease of $I_C R$, in comparison with the effective energy gap, with increasing Ta layer thickness is observed. In addition, we have employed a modified version of the Gallagher theory¹ including strong-coupling and electron-scattering effects to self-consistently fit both the bound state energy and $I_C R$ product as a function of D_{Ta} , over a wide range of overlayer thicknesses.

A study of the oxidation properties of Ta overlayer and other systems reveals a general empirical dependence of barrier height with width of the form $\bar{\phi} \sim 6\text{eV}/(s - 10\text{\AA})$. A representative description of the data can be obtained from the Fromhold-Mott-Cabrera² theory of self-limiting oxide growth on metals, although at present a definitive evaluation of the association between measured and thickness-determining barrier shape is precluded in part by a lack of detailed information concerning the oxide/counter-electrode interface.

Acknowledgements

The authors would like to thank M.R. Beasley, M. Gurvitch, J.M. Rowell, and W.J. Tomasch for many useful discussions. This work was supported by NSF ECS-83-05000, NSF DMR-80-19739 and ONR N00014-80-C-0855.

References

1. W.J. Gallagher, *Physica* **108B**, 825 (1981).
2. A.T. Fromhold, Jr. *Theory of Metal Oxidation*, Vol. 1; (North-Holland Publishing Co., New York, 1976), N. Cabrera and N.F. Mott, *Rept. Progr. Phys.* **12**, 163 (1949).
3. S.T. Ruggiero, D.W. Face, and D.E. Prober, *IEEE Trans. Magn.* **MAG-19**, 960 (1983).
4. S.T. Ruggiero, G.B. Arnold, E. Track and D.E. Prober, in *Proceedings of the 17th Int. Conf. on Low Temperature Physics*, 1984 (to be published).
5. E.L. Wolf, J. Zadazinski, J.W. Osmun, and G.B. Arnold, *J. Low Temp. Phys.* **40**, 19 (1980).
6. M. Gurvitch, M.A. Washington, and H.A. Huggins, *Appl. Phys. Lett.* **42**, 472 (1983).
7. C.P. Umbach, A.M. Goldman, and L.E. Toth, *Appl. Phys. Lett.* **40**, 81 (1982).
8. J. Kwo, G.K. Wertheim, M. Gurvitch, and D.N.E. Buchanan, *IEEE Trans. Magn.* **MAG-19**, 795 (1983).
9. S. Celaschi, R. Hammond, T.H. Geballe, W.P. Lowe, and A. Green, *Bull. Am. Phys. Soc.* **28**, 423 (1983).
10. G.B. Arnold, *Phys. Rev.* **B18**, 1076 (1978); E.L. Wolf and G.B. Arnold, *Phys. Reports* **91**, 31 (1982).
11. R.C. Dynes and J.M. Rowell, *Phys. Rev.* **B11**, 1884 (1975).
12. L.N. Smith, J.B. Thaxter, D.W. Jillie, and H. Kroger, *IEEE Trans. Magn.* **MAG-18**, 1571 (1982).
13. J.M. Rowell, W.L. McMillan, R.C. Dynes, (to be submitted to the *Journal of Chemical and Physics Reference Data*).
14. S. Celaschi, T.H. Geballe and W.P. Lowe, *Appl. Phys. Lett.* **43**, 794 (1983).
15. D.W. Face, et al. (in preparation).
16. D.G. Walmsley, E.L. Wolf, J.W. Osmun, *Thin Solid Films* **62**, 61 (1979).
17. M.A. Ocampo, J.L. Heiras, and T.A. Will, *J. Appl. Phys.* **53**, 3698 (1982).
18. J.M. Rowell, in *Tunneling Phenomena in Solids*, Eds. E. Burstein and S. Lundquist (Plenum, New York, 1969).
19. J.M. Rowell, M. Gurvitch, and J. Geerk, *Phys. Rev.* **B24**, 2278 (1981).
20. W.F. Brinkman, R.C. Dynes, and J.M. Rowell, *J. Appl. Phys.* **41**, 1915 (1970).
21. See Ref. 2 (A.T. Fromhold), eqs. 10.7, 10.54, and 10.59.
22. M.J. Dignam, W.R. Fawcett, and H. Bohni, *J. Electrochem. Soc.* **113**, 656 (1966).
23. D.A. Vermilyea, *Acta Metall.* **6**, 166 (1958).